Processing and Application of Ceramics 9 [2] (2015) 67–71

DOI: 10.2298/PAC1502067P

Annealing effects on the properties of TiN thin films

Maja Popović*, Mirjana Novaković, Nataša Bibić

University of Belgrade, "Vinča" Institute of Nuclear Sciences, P.O. Box 522, 11001 Belgrade, Serbia

Received 3 April 2015; Received in revised form 1 June 2015; Accepted 17 June 2015

Abstract

The structure, absorption coefficient and electrical resistivity studies on TiN thin films are presented. The film of thickness 240 nm was grown on Si (100) substrate by DC reactive sputtering at an average deposition rate of ~8 nm/min. After deposition the samples were annealed for 1 h at 600 °C and 2 h at 700 °C in nitrogen ambient and vacuum furnace, respectively. Structural characterizations were performed by Rutherford backscattering spectrometry (RBS), X-ray diffraction (XRD) and transmission electron microscopy (TEM). The optical properties were investigated by spectroscopic ellipsometry while a four point probe was used for electrical characterization. It was found that the post-deposition annealing of the films did not cause any variation in stoichiometry, but strongly affects the structural parameters such as lattice constant, micro-strain and grain size. The observed increase in the grain size after annealing leads to significantly lower value of the coefficient of absorption. These changes could be directly correlated with variation of electrical properties of TiN thin films.

Keywords: *titanium nitride, thin film, sputtering, annealing, TEM, RBS, XRD*

I. Introduction

Titanium nitride (TiN) is a well-known material which exhibits specific combination of physical, chemical, optical and mechanical properties like high hardness, abrasion and wear resistance, good thermal and chemical stability [1–4]. It is therefore widely applied in different field of industry, e.g. as a cutting, milling and drill tools coating [5], in micro- and nano-electronics like diffusion barriers, electrodes and Shottky contacts [6,7], in solar cells, optical filters [8–10]. Furthermore, titanium nitride exhibits a beautiful golden colour which makes this material interesting for decorative applications. This ceramic coating is generally produced by physical vapour deposition (PVD) [11,12], chemical vapour deposition (CVD) [13], ion beam assisted deposition (IBAD) [14] or hallow cathodic ionic plating [15]. Among them the deposition of TiN films by sputtering has important advantages such as low level of impurities and easy control of deposition rate. This method also enables the production of thin films with different morphology and crystal structure. It was found that the microstructure of TiN films is very sensitive to the deposition parameters and therefore controlled growth, composition and crystallographic orientation of TiN layers can significantly influence their properties [16].

Annealing process as an additional post-deposition thermal treatment can be widely used method to optimize the microstructure and then improve the physical properties of hard coatings by reducing the residual stresses and defects in the deposited films [17,18]. However, a literature review of TiN coatings reveals contradictory results on the change in microstructure after annealing. Chou *et al.* [19] have reported that the residual stress and hardness of ion-plated TiN films are decreased after heat treatment at 700 °C, while the microstructure inside the TiN films is not significantly changed. Mayrhofer *et al.* [20] investigated unbalanced magnetron sputtered TiN thin films for various deposition conditions. They have found that the annealing treatment shows a great effect on the grain size and crystallographic orientation in the nanocrystalline TiN films. Similar influence of heat treatment on the texture, grain size and crystallinity was found by Huang *et al.* [21]. This reveals that the structural evolution is controlled by thermal energy which facilitates the atom rearrangement diffusion in the films.

In the present study, DC reactive sputtered TiN thin films have been annealed at 600 and 700 °C, and the effects of heat treatment on the structural and optical

* Corresponding author: tel/fax: +381 11 6308 425,
e-mail: *majap@vinca.rs*

properties of the films are discussed. The changes in electrical properties induced by heat treatment are also included in this paper.

II. Experimental procedure

Titanium nitride thin films were deposited using DC reactive sputtering in the Balzers II Sputtron system. The sputtering target was pure titanium (99.9%) with diameter of 6 cm. Prior to deposition the chamber was evacuated to a base pressure of 1×10^{-4} Pa. Then high purity working gas argon and reactive gas nitrogen were introduced in the chamber to the partial pressure of 1×10^{-1} Pa and 3×10^{-2} Pa, respectively. Titanium nitride was-deposited at a rate of ~8 nm/min; the thickness of the film was fixed at about 240 nm by controlling the deposition duration. The film was-deposited on p-type (100) Si wafers thickness of 550 μm which were cleaned by chemical etching in a dilute hydrofluoric acid solution and then rinsed in deionized water. After deposition the samples were annealed at 600 °C for 1 h in the nitrogen atmosphere at a pressure of 2×10^{-2} Pa and at 700 °C for 2 h in a vacuum furnace at a pressure of 10^{-6} Pa.

The effect of annealing on the stoichiometry and microstructure of the produced films was studied using Rutherford backscattering spectrometry (RBS), X-ray diffraction (XRD) and transmission electron microscopy (TEM). The optical properties were probed by spectroscopic ellipsometry while four point probe method was used for electrical characterization. RBS measurements were performed using 900 keV He^{2+} ions at IONAS facility [22]. Random spectra at normal incidence were collected by two surface barrier detectors, positioned at ±165° scattering angle. The spectra were analysed using the Data Furnace Code [23]. X-ray diffraction was performed at a Philips PW1050 diffractometer with the CuK_α line in Bragg-Brentano geometry. TEM analysis was done on a JEOL 100CX and Philips CM30 electron microscopes operated at 100 kV and 300 kV, respectively. The samples were prepared for cross-sectional analysis by ion beam thinning. Also, micro-diffraction technique (MD) was used for the analysis the crystalline structure of the samples. Ellipsometry measurements were made using a Horiba JOBIN Yvon spectroscopic ellipsometer operating in the wavelength range of 260–2100 nm at an angle of incidence of 70°. Sheet resistance of the samples was measured by four point probe method.

III. Results and discussion

RBS measurements have been performed to determine the composition of TiN layers. The experimental RBS spectra taken from the TiN samples before and after annealing at 600 and 700 °C were presented in Fig.1a, while extracted depth profiles of the sample annealed at 600 °C are shown in Fig. 1b. From the experimental RBS spectra two well separated signals were observed for all three samples: one is on a position near 650 keV arising from Ti atoms while the other signal belongs to Si. The signal from N atoms, expected near backscattering energy of 250 keV, was overlapped with the signal arising from the substrate atoms. Compared with the as-deposited sample the spectra of post annealed samples remained essentially the same, which suggests that annealing did not induce any redistribution of components in TiN samples. The extracted depth profiles of sample annealed at 600 °C (Fig. 1b) show nearly uniform concentration of Ti and N over the full depth of the sample hinting at existence of TiN phase after annealing. As also shown in this figure, the annealed sample contain the argon ions in the concentration of approximately 1.5 at.%, which is incorporated in the layer during the deposition process. The extracted atomic concentrations of Ti, N and Ar for the as-deposited and annealed TiN layers are given in Table 1.

The as-deposited and annealed TiN samples were further analysed by XRD (Fig. 2). In the case of the

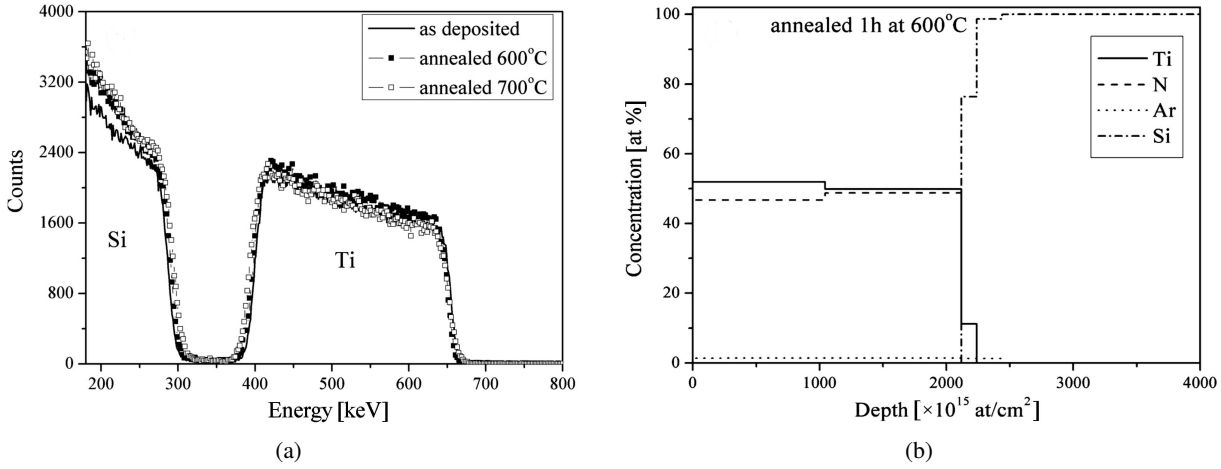

Figure 1. RBS experimental spectra taken from as-deposited TiN sample, sample annealed 1 h at 600 °C in N_2 atmosphere and sample annealed 2 h at 700 °C in vacuum (a) and extracted depth profiles of sample annealed 1 h at 600 °C in N_2 atmosphere (b)

Table 1. Compositions of TiN samples obtained by RBS analyses

Sample	Ti [at.%]	N [at.%]	Ar [at.%]	Ti/N
As deposited	49.8	48.1	2.1	1.04
Annealed at 600 °C	51.4	47.1	1.5	1.09
Annealed at 700 °C	50.4	48.2	1.4	1.04

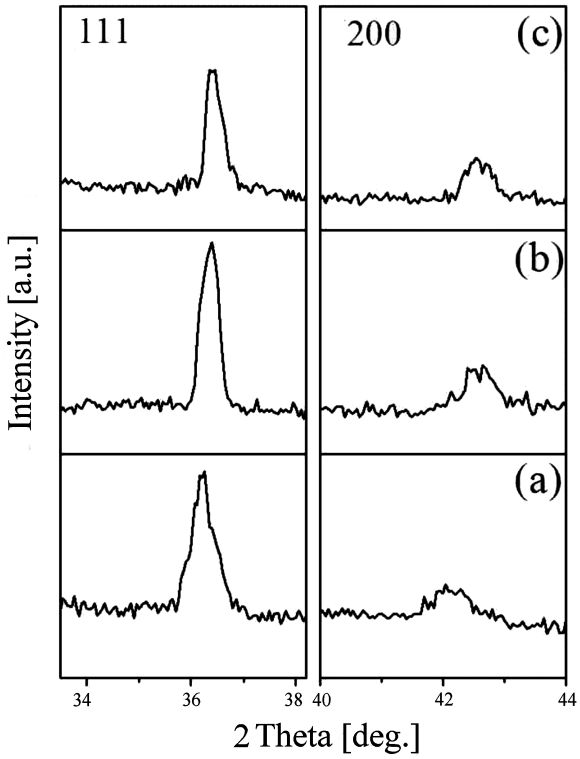

Figure 2. XRD diffraction peaks of 111 and 200 from TiN layers: a) as-deposited, b) heat treated at 600 °C for 1 h in nitrogen atmosphere and c) heat treated at 700 °C for 2 h in vacuum

as-deposited sample (Fig. 2a) two peaks on the positions at 36.20° and 42.14° corresponding to the TiN cubic structure are detected giving a lattice parameter of 0.4295 nm. This value is very close to the value obtained in the literature [24] for TiN films. Also, it can be seen, from the intensity of the peaks, that the 111 line is more intense than the 200 one. After annealing at 600 and 700 °C (Figs. 2b,c) the crystallographic cubic structure is kept, 111 and 200 peaks belonging to TiN are shifted to larger angles, which means that the high temperature reduces the lattice parameter. We measured a = 0.4262 nm and 0.4259 nm for the sample annealed at 600 and 700 °C respectively, which represents about 1% contractions. Besides the shifting of the peaks, a decreasing of peaks width was observed as a result of decreasing stresses and reduction in the concentration of defects during annealing. The amount of recovery effects strongly depends on the driving force which arises from the energy stored in the grains. Also, the broadening of the 111 and 200 peaks was used to calculate the average grain size using Scherrer's equation [25]. It was found that the grain size for the TiN film annealed at 600 °C was 19 nm and increased to 22 nm in the case of the film annealed at 700 °C which is a result of subgrain growth and grain boundary migration which occurred during annealing. From the above analysis, the values of the lattice constants, mean grain size and micro-strain obtained for the as-deposited and annealed samples are summarized in Table 2.

To provide additional insight into the microstructure of the as-deposited and annealed TiN layers, we used the TEM and MD analyses. TEM dark-field image of the as-deposited TiN sample and bright field image of the sample annealed at 700 °C with respective MD patterns, are presented in Figs. 3a, and 3b, respectively. We observed polycrystalline columnar structure in the as-deposited TiN layer with clear columns (bright contrast on figure) that are a few tens of nm wide perpendicular to the surface of the Si wafer. Inset in Fig. 3a is a micro-diffraction taken from an area covering the whole TiN layer and partially Si substrate. The first three diffraction rings are labelled in figure and belong to 111, 200 and 220 Bragg reflections. The other rings belong to the higher order *hkl* reflections. Bright field image of sample annealed at 700 °C (Fig. 3b) also shows individual columns that stretch from the substrate to the surface which means no obvious differences in the structure between the as-deposited and annealed TiN sample. But, careful TEM investigation of electron diffraction (inset in Fig. 3b) and compared to the pattern shown in (Fig. 3a), showed a large number of bigger well separated spots lying on the circles around the central spot, indicating the presence of larger grains in the TiN sample after annealing. These results are in agreement with the results of XRD analysis which indicate bigger grains after annealing.

The optical properties of the as-deposited and annealed TiN films were investigated using spectroscopic ellipsometry. In this technique two values are used to

Table 2. The lattice constant, micro-strain, grain size and electric resistivity of as-deposited and annealed TiN thin films

Sample	a [nm]	ε ($\times 10^{-3}$)	D [nm]	Electric resistivity [$\mu\Omega$ cm]
As deposited	0.4295	2.425	15	73.3
Annealed at 600 °C	0.4262	1.92	19	63.4
Annealed at 700 °C	0.4259	1.72	22	55

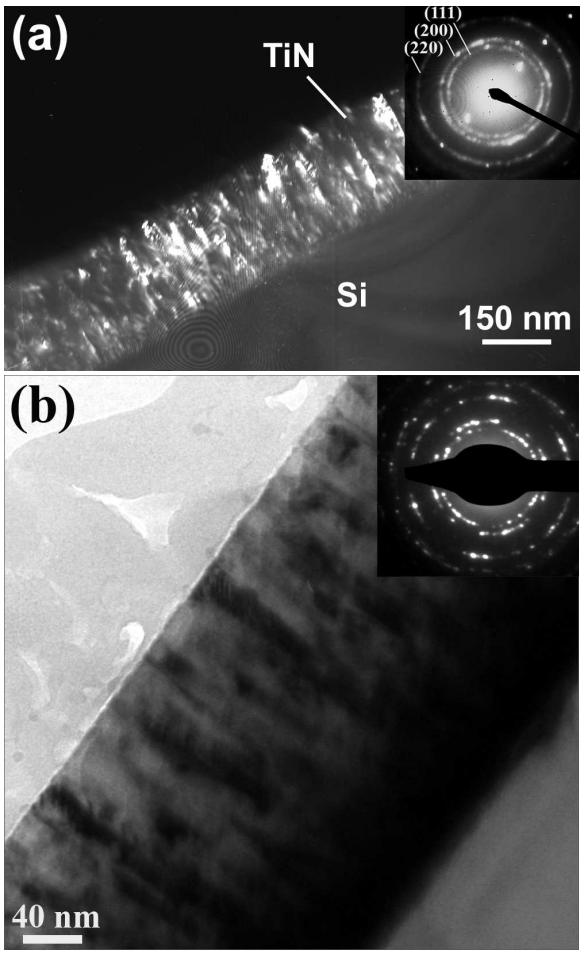

Figure 3. TEM analysis and corresponding MD patterns of TiN layers: a) dark field image of as-deposited sample and b) bright field image of the sample annealed at 700 °C for 2 h in vacuum

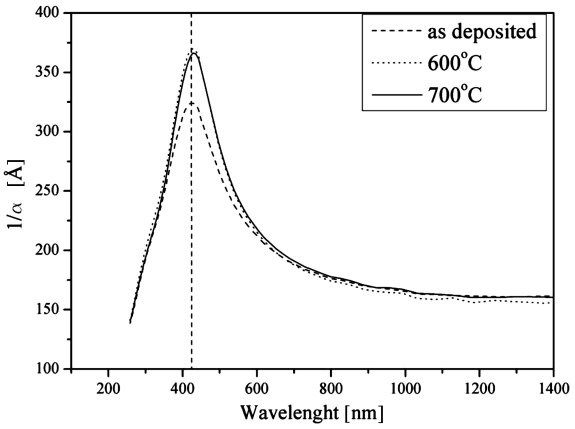

Figure 4. $1/\alpha$ versus wavelength for as-deposited and annealed TiN films

describe the optical properties which determine how light interacts with a material. They are generally represented as a complex numbers and consist of the index refraction (n) and extinction coefficient (k). Extinction coefficient k determines how fast light disappears in the medium and is related to absorption coefficient α through relation $\alpha = 4\pi k/\lambda$. From the extinction coefficient the wavelength profiles of the inverse of the absorption coefficient $1/\alpha$, for the as-deposited and annealed samples, have been derived and are shown on Fig. 4. It was found that the annealed TiN films exhibited similar $1/\alpha$ spectral behaviour compared to the as-deposited film. Maximum values of $1/\alpha$ of the as-deposited TiN sample and those annealed at 600 and 700 °C were 324.1, 370.1 and 366.3 Å, respectively, indicating a significant increase in this value in the visible range of spectra after annealing. This practically means that the absorption coefficient decreased after annealing which corresponds to a smaller absorption in this range of spectra. These changes can be explained due to reducing the defect content and stress relaxation in the films during heat treatments. The formation of larger grains at higher temperature, as confirmed by XRD and TEM, may be also responsible for the decrease of absorption coefficient.

The influence of annealing on the electrical characteristics of TiN films was analysed by measuring the sheet resistance by standard four point probe technique at room temperature. It was found that the as-deposited film showed higher electrical resistivity than those annealed at 600 and 700 °C (Table 1). Obviously, the increase of annealing temperature results in lower defect density, vacancies or interstitials in TiN thin films which leads to decreasing in electrical resistivity. The behaviour of resistivity is in agreement with the registered increase of the grain size upon annealing.

IV. Conclusions

Stoichiometric single phase *fcc* TiN thin film has been deposited via DC reactive sputtering and then subjected to annealing treatments at 600 and 700 °C. The influence of the annealing treatment on the microstructure, absorption coefficient and resistivity was investigated. After heat treatment, the stoichiometry of the films is not significantly changed. But, the results show that the annealing induces changes in lattice constant, grain size, micro-strain, coefficient of absorption and resistivity in TiN films. For the annealing temperature at 600 and 700 °C we register a decrease in lattice constant and micro-strain in the film and an increase of the grain size. These changes in structural parameters are responsible for the decrease of absorption coefficient and electrical resistivity in annealed TiN films.

Acknowledgements: This work was supported by the Ministry of Education and Science of the Republic of Serbia (Project No. III 45005) and by Deutsche Forschungsgemeinschaft (Project 436 SER 113/2).

References

1. D. Gall, S. Kodambaka, M.A. Wall, I. Petrov, J.E. Greene, "Pathways of atomistic processes on TiN (001) and (111) surfaces during film growth: An ab initio study", *J. Appl. Phys.*, **93** (2003) 9086–9094.

2. J.E. Sundgren, "Structure and properties of TiN coatings", *Thin Solid Films*, **128** (1985) 21–44.
3. R.R. Manory, S. Mollica, L. Ward, K.P. Purushotham, P. Evans, J. Noorman, A.J. Perry, "The effects of MEVVA ion implantation on the tribological properties of PVD-TiN films deposited on steel substrates", *Surf. Coat. Technol.*, **155** (2002) 136–140.
4. P. Patsalas, S. Logothetidis,"Optical, electronic, and transport properties of nanocrystalline titanium nitride thin films", *J. Appl. Phys.*, **90** (2001) 4725–4734.
5. D.A. Glosker, S.I. Shah, *Handbook of Thin Film Process Technology 2*, IOP Publishing, Bristol and Philadelphia, 1995.
6. L. Gao, J. Gstöttner, R. Emling, M. Balden, Ch. Linsmeier, A. Wiltner, W. Hansch, D. Schmitt-Landsiedel, "Thermal stability of titanium nitride diffusion barrier films for advanced silver interconnects", *Microelectron. Eng.*, **76** (2004) 76–81.
7. M. Moriyama, T. Kawazoe, M. Tanaka, M. Murakami, "Correlation between microstructure and barrier properties of TiN thin films used Cu interconnects", *Thin Solid Films*, **416** (2002) 136–144.
8. N. Kalfagiannis, S. Logothetidis, "Color dependency on optical and electronic properties of TiN_x thin films", *Rev. Adv. Mater. Sci.*, **15** (2007) 167–172.
9. G.M. Matenoglou, S. Logothetidis, S. Kassavetis, "Durable TiN/TiN_x metallic contacts for solar cells", *Thin Solid Films*, **511-512** (2006) 453–456.
10. S. Venkataraj, D. Severin, S.H. Mohamed, J. Ngaruiya, O. Kappertz, M. Wuttig, "Towards understanding the superior properties of transition metal oxynitrides prepared by reactive DC magnetron sputtering", *Thin Solid Films*, **502** (2006) 228–234.
11. I. Petrov, L. Hultman, U. Helmersson, J.-E. Sundgren, J.E. Greene, "Microstructure modification of TiN by ion bombardment during reactive sputter deposition", *Thin Solid Films*, **169** (1989) 299–314.
12. T.-S. Kim, S.-S. Park, B.-T. Lee, "Characterization of nano-structured TiN thin films prepared by R.F. magnetron sputtering", *Mater. Lett.*, **59** (2005) 3929–3932.
13. Y.W. Bae, Y.W. Lee, T.S. Bessman, T.J. Blau, "Nanoscale hardness and microfriction of titanium nitride films deposited from the reaction of tetrakis (dimethylamino) titanium with ammonia", *Appl. Phys. Lett.*, **65** (1995) 1895–1896.
14. K. Yokota, K. Nakamura, T. Kasuya, S. Tamura, T. Sugimoto, K. Akamatsu, K. Nakao, F. Miyashita, "Relationship between hardness and lattice parameter for TiN films deposited on SUS 304 by an IBAD technique", *Surf. Coat. Technol.*, **158-159** (2002) 690–693.
15. W.-J. Chou, G.-P. Yu, J.-H. Huang, "Deposition of TiN thin films on Si(100) by HCD ion plating", *Surf. Coat. Technol.*, **140** (2001) 206–214.
16. G. Abadias, "Stress and preferred orientation in nitride-based PVD coatings", *Surf. Coat. Technol.*, **202** (2008) 2223–2235.
17. W. Mader, H.F. Fischmeister, E. Bergmann, "Defect structure of ion-plated titanium nitride coatings", *Thin Solid Films*, **182** (1989) 141–152.
18. X. Kewei, C. Jin, G. Rensheng, H. Jiawen, "Thermal effects of residual macrostress and microstrain in plasma-assisted CVD TiN films", *Surf. Coat. Technol.*, **58** (1993) 37–43.
19. W.-J. Chou, G.-P. Yu, J.-H. Huang, "Effect of heat treatment on the structure and properties of ion-plated TiN films", *Surf, Coat. Technol.*, **168** (2003) 43–50.
20. P.H. Mayrhofer, F. Kunc, J. Musil, C. Mitterer, "A comparative study on reactive and non-reactive unbalanced magnetron sputter deposition of TiN coatings", *Thin Solid Films*, **415** (2002) 151–159.
21. J.-H. Huang, K.-J. Yu, P. Sit, G.-P. Yu, "Heat treatment of nanocrystalline TiN films deposited by unbalanced magnetron sputtering", *Surf. Coat. Techol.*, **200** (2006) 4291–4299.
22. M. Uhrmacher, K. Pampus, F.J. Bergmeister, D. Purschke, K.P. Lieb, "Energy calibration of the 500 kV heavy implanter ionas", *Nucl. Instr. Meth. B*, **9** (1985) 234–242.
23. N.P. Barradas, C. Jeynes, R.P. Webb, "Simulated annealing analysis of Rutherford Backscattering data", *Appl. Phys. Lett.*, **71** (1997) 291–293.
24. E. Cerro Prada, V. Torres Costa, P. Herrero, G. Ceccone, M. Manso-Silvan, "Interface between cement paste and thin TiN film for corrosion resistance enhancement; structural, morphological and electrochemical properties", *Constr. Build. Mater.*, **80** (2015) 48–55.
25. B.D. Cullity, *Elements of X-ray diffraction*, Wokingham: Addison-Wesley, 1967.